Analysis of Low-Cycle Fatigue at Notches in a Single Crystal Superalloy at High Temperature

P. Boubidi and R. Sievert

Federal Institute for Materials Research and Testing (BAM)
Unter den Eichen 87, D-12200 Berlin, Germany
e-mail: Pascal.Boubidi@bam.de, Rainer.Sievert@bam.de

Abstract

The inelastic behaviour at notches in SC16 single crystals at 950 ^{o}C has been calculated using a three-dimensional crystallographic viscoplastic model. For a $\langle 001 \rangle$ oriented round specimen with a circumferentially V-shaped notch, the highest equivalent inelastic strain cumulated in each of the two slip families, octahedral and cubic, arises for cubic slip systems. This maximum equivalent slip is located not directly at the notch root, instead it is shifted a little away from there. Fractographic observations show, that a similar shifting is present for the occurence of the main cracks. This inhomogeneity of the stress-strain situation at notches in single crystals is taken into account at the definition of a lifetime parameter based on the resolved shear stresses.

Short Introduction

In a gas turbine blade, LCF life controlling notches are given by film cooling holes which are required to form a thin film of cooling air on the surface [9]. On the other hand, a considerable data base has been performed in a previous gas turbine project at the BAM [12] on smooth specimens of the single crystalline model material SC16 with different orientations especially at 950 ^{o}C. Therefore, the present investigation of the low-cycle fatigue (LCF) at notches in single crystals at high temperature is build up on that data base for SC16.

Material and Experimental Procedure

The two phases nickel base superalloy SC16 is obtained after heat treatment and the microstructure consists of 35 % cuboidal γ' particles with a mean edge length of 450 nm and about 5 % spherical particles with a mean diameter of 80 nm [6].
At 950^{o}C and on air constant strain amplitude fatigue tests with zero mean strain were performed at uniaxial loading on smooth specimens with 9 mm diameter in the gauge length as well as on circumferentially notched round specimens. The root of the V-shaped notch had two different radii, 0.2 mm and 1 mm. The global strain amplitude measured by the extensometer with a 21.5 mm gauge length over the notches was $\pm 0.15\%$.

Test	Notch radius (mm)	$\triangle\sigma_{\mathrm{Mises}}$ (MPa)	N_f
1	0.2	1508	120
2	0.2	1508	127
3	0.2	1508	131
4	1.0	966	583

Table 1: LCF tests on $\langle 001 \rangle$ oriented SC16 circumferentially notched round specimens at 950^{o}C.

The displacement control on notched specimens shall describe the important thermal strain control in gas turbine blades [9]. The strain rate was $10^{-3}\ s^{-1}$ for all the tests.
Usually we fixed the lifetime N_f at the number of cycles to 5% stress drop in tension with respect to a decreasing regression straight-line including points behind saturation. Except for the test 2, see table 1, which was performed until rupture and an interrupted one, we stopped the tests at 10% stress drop in tension. Some photomicrographs of the surface of these specimens were taken. Then the specimens were broken at room temperature. Some micrographs of their fracture surfaces were taken in order to characterize the crack growth mechanisms in the singles crystal for such geometries.

Experimental Results

Metallographic observations:

The fractographic observations of near ⟨001⟩ notched specimens (Fig. 1, 2) with a scanning electron microscope (SEM) show two main cracks which occured perpendicular to the external load, but indeed they arose not directely at the notch root, instead they are shifted a little away from there. For a near ⟨011⟩ oriented specimen the main cracks seem to be concentrated at the notch root.
The "square shape" of the crack front (Fig. 3, 4) allows us to assume that the cracks do not grow homogeneously in the depth. We drew the projection of the secondary crystallographic axes of the material on the micrographs of the fracture surfaces. The direction [100] seems to be close to the maximum crack growth in the depth.
Metallographic observations on a ⟨001⟩ notched specimen with 1 mm notch radius in an interrupted test showed a relatively late initiation of a crack within the lifetime, although the stresses are much higher at the notch surface. This seems to indicate the importance of the situation close to the surface in the single crystal, because when a crack is observable there, then the lifetime is reached not much later, at least at 1 mm notch radius.

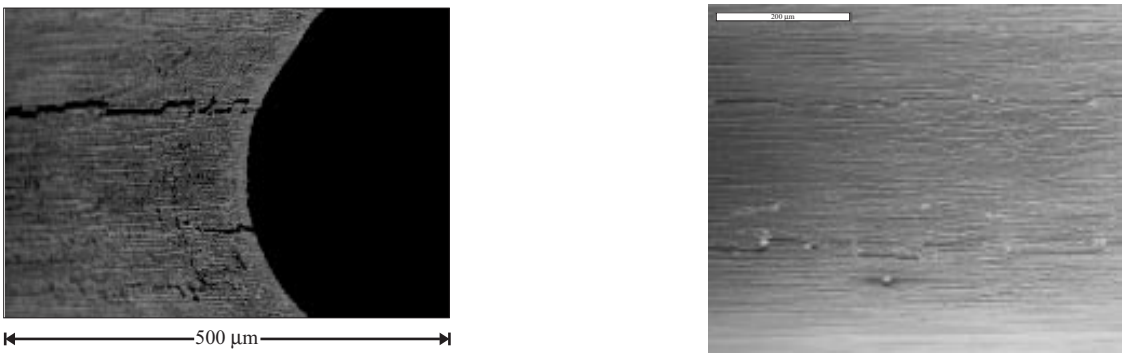

Figure 1: Notch of the ⟨001⟩ SC16 specimen 3 with 0.2 mm notch radius after N = 250 cycles at 950°C.

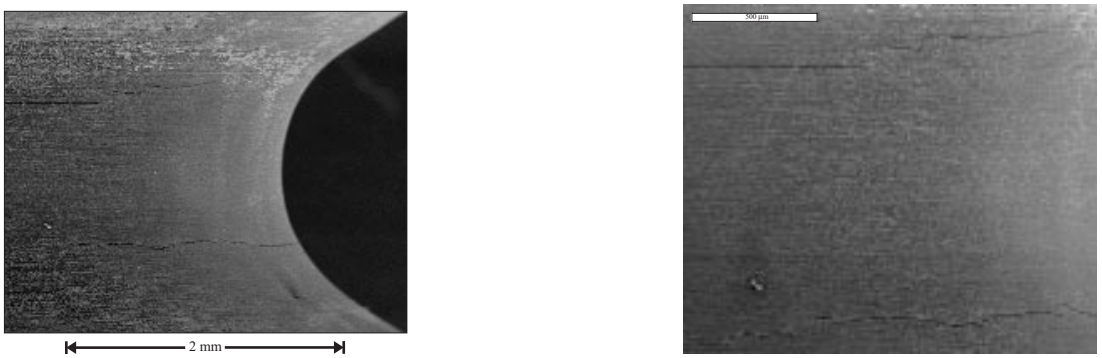

Figure 2: Notch of the ⟨001⟩ SC16 specimen 4 with 1 mm notch radius after N = 810 cycles at 950°C.

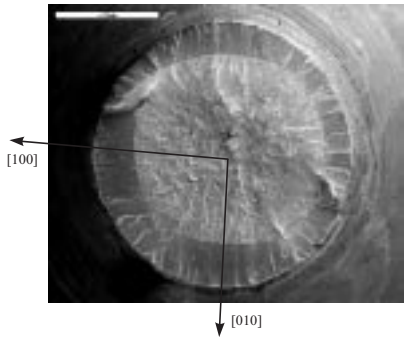

Figure 3: Fracture surface of the ⟨001⟩ SC16 specimen 1 with 0.2 mm notch radius after N = 275 cycles at 950^{o}C.

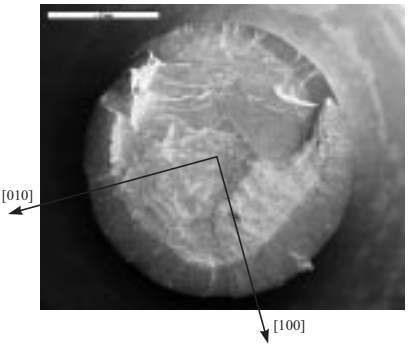

Figure 4: Fracture surface of the ⟨001⟩ SC16 specimen 4 with 1 mm notch radius after N = 810 cycles at 950^{o}C.

Fatigue life results:

A lot of axial strain controlled LCF tests at high temperature were already carried out at the BAM on SC16 smooth specimens [12]. Despite of the relatively scatter, the fatigue diagram at 950 ^{o}C and 10^{-3} s^{-1} strain rate, Fig. 5 (above), shows essentially no dependence of the lifetime on the orientation of the single crystal at the same stress range as also found in [4]. Of course, the stresses itself arise in dependence on the crystal orientation. For example, at the same total strain range, the lifetime is lower for near ⟨011⟩ orientation as for near ⟨001⟩ orientation, but the stress range is higher at ⟨011⟩. Thus, we obtain within a scatter band a very simple assessment rule, see Fig. 5. It is noteworthy that the inelastic strain range increases, too, at ⟨011⟩ orientation due to the higher elastic stiffness (Young's modulus) in this direction.

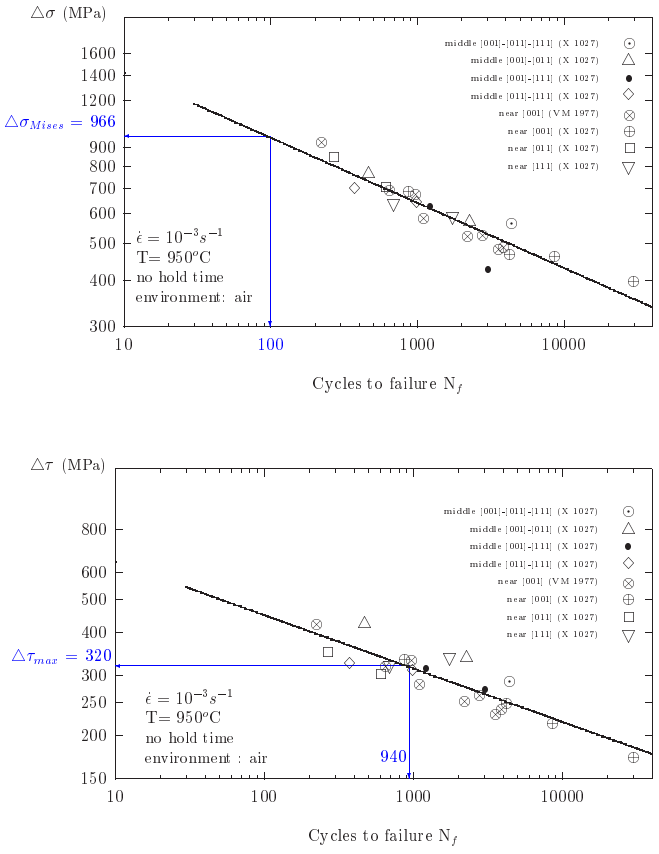

Figure 5: Experimental fatigue life for different orientations depending on the axial stress range (above) and on the maximum resolved shear stress range simulated (below) for the single crystal superalloy SC16 at uniaxial loading for different charges (X,VM). The maximum Mises stress range $\triangle\sigma_{\mathrm{Mises}}$ in the ⟨001⟩ specimen with 1 mm notch radius (above) and the maximum resolved shear stress range $\triangle\tau_{\mathrm{max}}$ at maximum equivalent slip in that specimen (below) are inserted.

The number of cycles to failure of the notched specimens are given in table 1. The maximum equivalent Mises stress range at the notch is calculated by FE method for the stabilized cycle. The tested notched specimens lived significantly longer than the smooth ones at the same maximum Mises stress at the notch. Compare, for example, the lifetime at maximum Mises stress range in the $\langle 001 \rangle$ specimen with 1 mm notch radius, Fig. 5 (above), with the experimentally obtained lifetime for that specimen 4 given in table 1.

Finite Element analysis of the LCF tests in the framework of crystal plasticity

Presentation of the model and identification of the parameters:

For single crystals the viscoplastic deformation results of the effects of dislocation motion on crystallographic planes by slip processes:

$$\underset{\sim}{\dot{\epsilon}}^{p} = \sum_{g=1}^{18} \dot{\gamma}^{g} \, {}^{s}(\underline{\mathbf{l}}^{g} \otimes \underline{\mathbf{n}}^{g}) \tag{1}$$

Where $\underline{\mathbf{l}}^{g}$ and $\underline{\mathbf{n}}^{g}$ respectively are the slip direction and the normal to the slip plane of slip system g which define the symmetric second order tensor. As at room temperature [3], we consider both octahedral (twelve) and cubic (six) slip systems at high temperature. We used the same approach of the constitutive equations written for small deformation and given in [7]:

$$\dot{\gamma}^{g} = \left\langle \frac{|\tau^{g} - x^{g}| - r^{g}}{k} \right\rangle^{n} \operatorname{sign}(\tau^{g} - x^{g}) \tag{2}$$

$$r^{g} = r_{o}^{g} + q^{g} \left(1 - e^{-bv^{g}}\right) \tag{3}$$

$$\dot{x}^{g} = |\dot{\gamma}^{g}| \, (c \, \operatorname{sign}(\dot{\gamma}^{g}) - d \, x^{g}) \tag{4}$$

We will call equivalent slip cumulated in a slip family G, the following quantity: $\sum_{g \in G} v^{g}$, where v^{g} is the cumulated slip of the slip system g. The material has an elastic behaviour with cubic symmetry until the distance computed from the resolved shear stress τ^{g} and the kinematic hardening variable x^{g} reaches the critical resolved shear stress r^{g} of the slip system g.

slip family	k MPa	n	r_o MPa	q MPa	b	c MPa	d
Octahedral	700	4.7	4.6	3.9	3.7	96536	1050
Cubic	1172	2.4	17.3	-4.4	2.7	77081	1056

Table 2: Material constants of SC16 at 950^{o}C.

An analysis of monotonic and cyclic behaviour of SC16 smooth specimens at 950^{o}C and at different orientations shows the necessity to take into account the local kinematic hardening and the viscosity. These observations confirm the ones already done for single crystal nickel base superalloys [7]. From a large experimental data base available at the BAM (tests for different orientations and strain rates) we calibrated the viscosity (k, n) and the hardening parameters (c, d, r_{o}^{g}, q^{g}, b) for each slip family with a classical technique of numerical optimization process [10]. We give in table 2 the constants of the model implemented in the FE program ZéBuLoN [5].

Model predictions and confrontation with the experimental results:

Conditions of the FE analysis

We give in this section the results of the calculations of two notched specimens used for the LCF tests with a notch radius of 0.2 mm and 1 mm. We performed the finite element calculations for the single crystal ideally ⟨001⟩ oriented to reduce the size of the problem. It is particularly the case for our LCF tests specimens which deviation of the [001] crystallographic axis is within 5^o. Moreover, due to the cubic symmetry, we only need to mesh one eighth of the structure, which is of the length of the extensometer. The mesh of the 0.2 mm (respectively 1 mm) notched radius specimen has 642 (respectively 690) isoparametric and quadratic elements. The LCF tests have been carried out with displacement control and we prescribed in the calculations the displacement of the extremity of the structure in order to describe the experimental value at the location of the extensometer: $\pm 0.15\%$ displacement amplitude related to the gauge length of the extensometer and $10^{-3}\ s^{-1}$ as its rate.

Viscoplastic stress-strain behaviour at notches

Contrary to the results of a uniaxial test of a ⟨001⟩ single-crystal smooth specimen, the presence of the notch activates both slip system families (Fig. 6, 7). The equivalent strain of the cubic slip is higher as the one of the octahedral slip and it is not located exactly at the notch root. The curves given in Fig. 10 represent the variation of them along the circumference too. The variable r is the radial coordinate starting at the notch root describing the line on the curved notch surface over the radius at a certain circumferential coordinate. They give a more precise idea of the weak variation of the equivalent inelastic strain along the circumference.

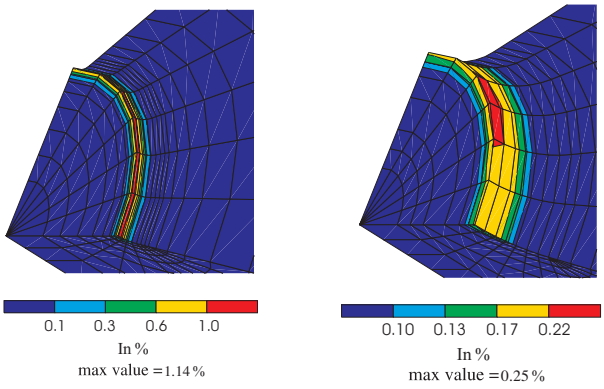

Figure 6: Equivalent slip for the octahedral slip system for two notch radii (0.2 mm (left) and 1 mm (right)) of a ⟨001⟩ specimen.

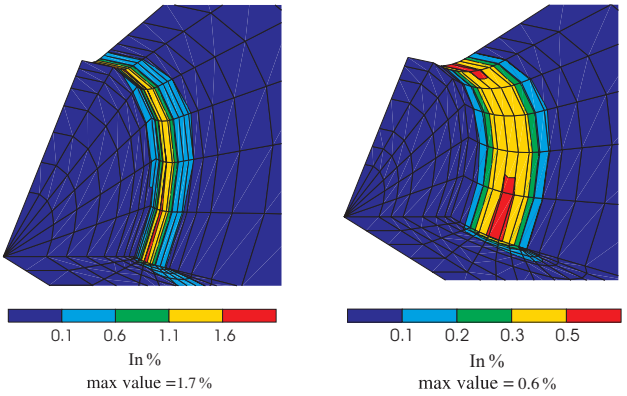

Figure 7: Equivalent slip for the cubic slip system for two notch radii (0.2 mm (left) and 1 mm (right)) of a ⟨001⟩ specimen.

Calculations of torsionally loaded tubular specimens have shown the inhomogeneity of the viscoplastic strain along the circumference [7]. More recently at the BAM it was confirmed with experimental results and even for tension-torsion tests the good agreement between the FE model and the local measurements at room temperature [3].
Due to the complex state of stress in the notch configuration within the single crystal a similar inhomogeneity of the strain is expected at a notch according to the model. Unfortunately it is impossible to use the same local measurement, on one hand because of the high temperature and on the other hand because of the geometry. If we take the maximum equivalent slip as relevant variable for the crack initiation at the surface and if we take into account the relative precision of its location's measurement, the experimental results are in accordance with the FE analysis, see Fig. 8, 9.

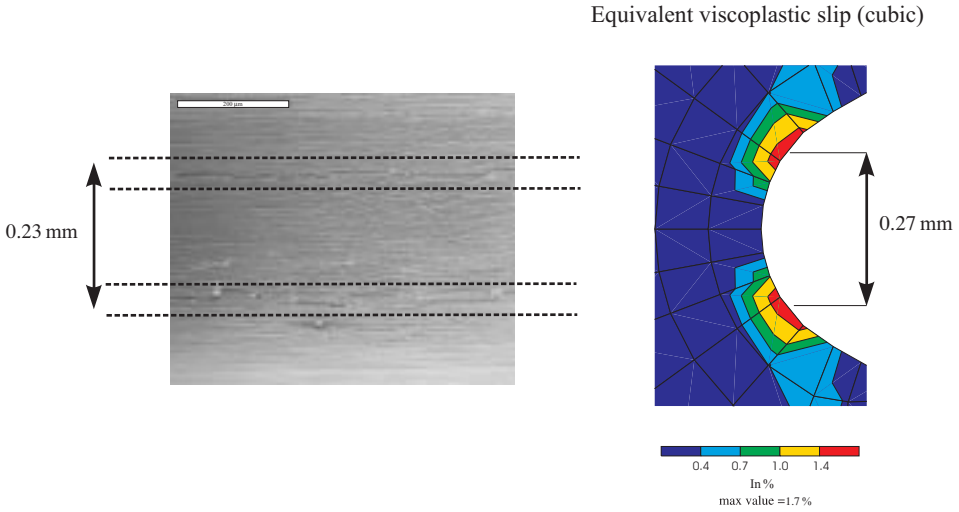

Figure 8: Comparison Experiment (Fig. 1) - FE simulation. Specimen 3 with 0.2 mm notch radius.

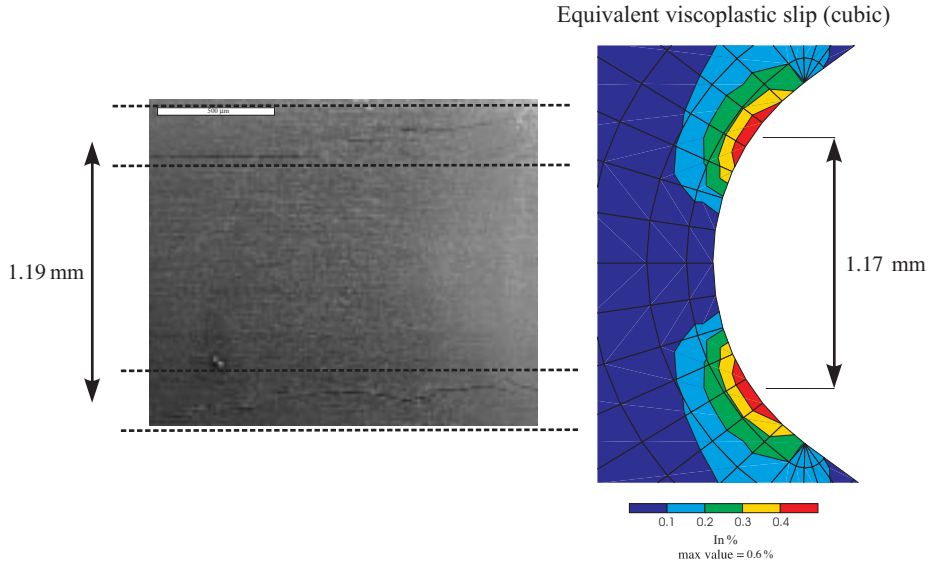

Figure 9: Comparison Experiment (Fig. 2) - FE simulation. Specimen 4 with 1 mm notch radius.

A lifetime parameter for LCF at notches in single crystals

The tested notched specimens lived significantly longer than the smooth ones at the same maximum Mises stress, see table 1 and Fig. 5 (above). This notch effect is usually observed [2]. That means that the maximum value at least of this equivalent stress alone can not give the fatigue life at notches. Moreover, the experimental results for the location of the macro-cracks described in the previous section indicate us to take into account in the lifetime assessment rule the full inhomogeneity of the strain and stress situation on the surface.
The *resolved shear stresses* on such slip systems, which represent not the full stress state but are *physical components* of it, are the more adequate loading quantities for a crystal. Thus, a possible choice of critical variable for damage is to take *at the point of maximum equivalent slip, the value of the maximum resolved shear stress for this slip family.*
For example we give in Fig. 11 the distribution of the resolved shear stress for the cubic slip along the circumference of the 1 mm notch radius specimen at the loading amplitude of the first cycle where SC16 at 950^{o}C is already cyclic saturated essentially. The origin of the angle corresponds to the point which is in the plane [100] and where the equivalent cubic slip is maximum, Fig. 10.
Thus we have a maximum resolved shear stress range of about 320 MPa. This stress is not the highest resolved shear stress at the inhomogeneously strained notch. It is strongly determined by the

anisotropy of the material. On the other hand we simulated all the LCF tests given in Fig. 5 for a homogeneous volume element. From that we obtained their maximum resolved shear stress ranges, taken from the 18 values of the two slip families (cubic and octahedral), versus the number of cycles to failure (Fig. 5, below). Thus it is possible to draw a straigth line in this log-log representation if we assume that the scatter is acceptable. If we report the value of the critical damage variable in this fatigue diagram we assess a lifetime of about 940 cycles which is within a factor of 2 compared to the experimental lifetime of 583 cycles for this 1 mm notch radius specimen given in table 1. The assessed lifetime at 0.2 mm notch radius is lower than the experimental one within a factor of 2.5. As a result, the number of cycles to failure of the performed LCF tests on notched specimens are comparable to the lifetimes of smooth specimens at the same maximum resolved shear stress value at maximum equivalent slip.

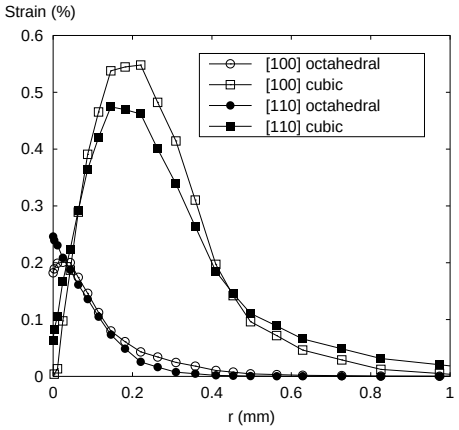

Figure 10: Equivalent slip for each slip system family on the surface of the notch (radius 1 mm) at two circumferential coordinates, [100] and [110].

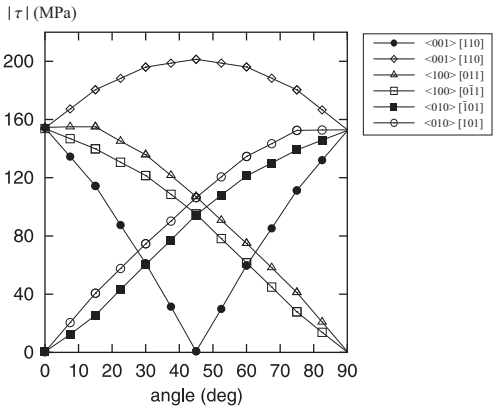

Figure 11: Resolved shear stresses along the circumference of the 1 mm notch radius specimen at the axial height of maximum inelastic strain of one slip family, i.e. of cubic slip. The angle of 0^o corresponds to the [100] secondary crystallographic axis.

Besides the inhomogeneity of resolved shear stresses and slip on the surface, decreasing stresses behind the notch root are present within a critical volume for crack initiation. [1] has already suggested that such stress gradient should be taken into account. A gradient dependent criterion for high-cycle fatigue was developed in [8]. So, one can put forward the same idea to low-cycle fatigue and single crystals in order to include in lifetime assessment the influence of the small size of the highly loaded volume at sharp notches on the lifetime.

Conclusion

In strain-controlled uniaxial LCF tests on SC16 smooth specimens at different orientations, 950 ^{o}C and 10^{-3} s^{-1} strain rate, essentially no dependence of the fatigue lifetime on the orientation was found at the same stress range.
Fractographic observations on $\langle 001 \rangle$ oriented notched specimens showed that the main cracks are located not directly at the notch root, instead they are shifted a little away from there. This corresponds to the similarily shifted maximum equivalent slip that is cumulated on cubic slip systems according to the numerical analysis.
The lifetimes of the performed LCF tests on notched single crystal specimens can be assessed from the cycles to failure of the smooth specimens taking as lifetime parameter the maximum resolved shear stress value present at the location of maximum equivalent slip in the notch.

Acknowledgement

This work has been supported by the European Community within the Brite-EuRam project BE96-3311. The contributions of the laboratory for mechanical testing (V.21, head: Dr. Klingelhöffer) and of the laboratory for electron microscopy (V.12, head: Dr. Österle) at the BAM are gratefully acknowledged. Furthermore, the authors would like to thank very much Dr. Bischoff-Beiermann of Siemens (KWU) as well as Prof. Cailletaud and Dr. Forest of the Centre des Matériaux de l'Ecole des Mines de Paris for helpful discussions.

References

[1] Chaudonneret M., Chaboche J. L., *"Fatigue life prediction of notched specimen"*, in: Fatigue of Engineering Materials and Structures, Inst. Mech. Eng., London, Vol. II, C296/86, p 503-510, 1986.

[2] Defresnes A., Rémy L., *"Fatigue behaviour of CMSX 2 superalloy [001] single crystal at high temperature, part I: Low cycle fatigue of notched specimens"*, Mat. Sc. and Eng., A129, p 45-53, 1990.

[3] Forest S., Olschewski J., Ziebs J., Kühn H.-J., Meersmann J., Frenz H., *"The elastic/plastic deformation behaviour of various oriented SC16 single-crystals under combined tension/torsion fatigue loading"*, in: Proceedings of the Sixth International Fatigue Congress, G. Lütjering and Nowack, Pergamon, pp. 1087-1092, 1996.

[4] Fleury E., *"Endommagement du superalliage monocristallin AM1 en fatigue isotherme et anisotherme"*, Ph.D. Dissertation, Ecole Nationale Supérieure des Mines de Paris, 1991.

[5] Foerch R., Besson J., Cailletaud G., Pilvin P., *"Polymorphic constitutive equations in finite element codes"*, comput. Methods Appl. Mech. Engrg., 141, pp. 355-372, 1997.

[6] Jiao F., Bettge D., Österle W., Ziebs J., Acta Mater., 44, 3933, 1996.

[7] Méric L., Cailletaud G., Poubanne P., *"Single Crystal Modeling for Structural Calculations"*, J. Engng. Materials and Technology: Part 1,2, vol. 113, pp. 162-182, 1991.

[8] Papadopoulos I. V., Panoskaltsis V. P., *"Invariant Formulation of a Gradient Dependent Multiaxial High-Cycle Fatigue Criterion"*, Engng. Fracture Mechanics, vol. 55, 4, pp. 513-528, 1996.

[9] Pan Y., Bischoff-Beiermann B., Schulenberg T., *"Material testing for fatigue design of heavy-duty gas turbine blading with film cooling"*, Fatigue Design and Reliability, G. Marquis and J. Solin (Eds), ESIS Publication 23, Elsevier, 1999.

[10] Cailletaud G., Pilvin P., *"Identification and inverse problems: a modular approach"*, ASME, MD-Vol 43, Material Parameter Estimation for Modern Constitutives Equations, Ed: L. A. Bertram, S. B. Brown and A. D. Freed, Book No. H00848, 1993.

[11] Telesman J., Ghosn L. J., *"Fatigue crack growth behaviour of PWA 1484 single crystal superalloy at elevated temperatures"*, ASME Paper 95-GT-452, 1995.

[12] Wedell W., Chrzanowski U., Frenz H., Ziebs J., Klingelhöffer H., *"Low cycle fatigue behaviour of the single crystal superalloy SC16."*, in: Proceedings of the Sixth International Fatigue Congress, G. Lütjering and Nowack, Pergamon, Vol. 2, pp. 807-812, 1996.